AIP Advances

RESEARCH ARTICLE | JANUARY 31 2024

On thermal performance of spine fin in magnetized hybrid fluid rooted with Cu and MoS_4 nanoparticles

T. N. Tanuja ; Kavitha L; Khalil Ur Rehman ; G. V. Kumar; Wasfi Shatanawi ; S. V. K. Varma ; Zeeshan Asghar

Check for updates

AIP Advances 14, 015068 (2024)
https://doi.org/10.1063/5.0176878

View Online
Export Citation
CrossMark

31 January 2024 17:57:00

AIP Advances
Why Publish With Us?
25 DAYS average time to 1st decision
740+ DOWNLOADS average per article
INCLUSIVE scope
Learn More
AIP Publishing

AIP Publishing

On thermal performance of spine fin in magnetized hybrid fluid rooted with Cu and MoS_4 nanoparticles

Cite as: AIP Advances 14, 015068 (2024); doi: 10.1063/5.0176878
Submitted: 18 September 2023 • Accepted: 8 January 2024 •
Published Online: 31 January 2024

View Online Export Citation CrossMark

T. N. Tanuja,[1,2] Kavitha L,[1] Khalil Ur Rehman,[3,a)] G. V. Kumar,[4] Wasfi Shatanawi,[3,5,a)] S. V. K. Varma,[1] and Zeeshan Asghar[3]

AFFILIATIONS

[1] Department of Mathematics, School of Applied Sciences, REVA University, Bengaluru, Karnataka, India
[2] Department of Mathematics, CHRIST (Deemed to be University), Bengaluru, India
[3] Department of Mathematics and Sciences, College of Humanities and Sciences, Prince Sultan University, Riyadh 11586, Saudi Arabia
[4] Department of Mathematics, CSSR and SRRM Degree and PG College, Kamalapuram 516289, Andhra Pradesh, India
[5] Department of Mathematics, Faculty of Science, The Hashemite University, P.O. Box 330127, Zarqa 13133, Jordan

[a)] **Authors to whom correspondence should be addressed:** kurrehman@psu.edu.sa and wshatanawi@psu.edu.sa

ABSTRACT

This study examines the thermal performance of diverse profiles of spine fins with variable thermal conductivity. A hybrid nanofluid comprising Cu, and MoS_4 with water as the base fluid, is modeled mathematically. Both the cylindrical and concave parabolic profiles are taken into account. The comparative outcomes are inferred from numerical and semi-analytical methods. The non-dimensional temperature profiles are analyzed graphically while considering the fin tip to be insulated, and the effects of various thermal parameters are also investigated. We have observed that the heat transfer rate shows an opposite trend toward convective-conduction and porosity parameter. The study also revealed that the concave parabolic profile emits more heat in comparison with the cylindrical profile.

© 2024 Author(s). All article content, except where otherwise noted, is licensed under a Creative Commons Attribution (CC BY) license (http://creativecommons.org/licenses/by/4.0/). https://doi.org/10.1063/5.0176878

I. INTRODUCTION

The most commonly used subject in engineering and technology is heat transfer. Many devices, such as refrigerators, boilers, and solar panels, are based on the principle of heat transfer. The mode of heat transfer includes different conduction, convection, and radiation. The enhancement of the rate of heat transfer plays a prominent role in the field of engineering and technology. This is due to the rapid development of various concepts and wide applications in this field. In the present situation, there is a need for compact devices that are efficient at transferring heat from devices to the surroundings, and hence, for this purpose, extended surfaces were introduced in the system. These extended surfaces are called "fins." Fins are considered to be an essential part of the devices and are most commonly equipped to enhance the heat emission rate of the concerned system. The extended surfaces exist in conventional applications such as air conditioning, refrigerators, motors, and generators.

Metals are used to prepare fins. Fins are available in various shapes. The important characteristic of fins that is noticed in this study is their diameter is always smaller than their length. The rate of enhancement of the heat transmission in a fin also depends on the geometry of the fin. Although classical fins such as rectangular fins, annular fins, and pin fins are applicable in the process of controlling the rate of heat transfer, adding an excessive number of these fins to the device makes no difference. Adding too many fins to the device restricts the free movement of air and, hence, reduces the convection heat transfer coefficient. Throughout the long term, the critical investigation of the fins leads to the revelation of the spine fin. Spine fins act as thousands of metal hairs on the condenser coil for effective removal of excess heat. They are encircled by the coil pipe, allowing the heat to be transferred to the airflow from all sides of the pipe.

Moradi and Ahmadikia[1] analytically studied the heat emission of quadrilateral, convex, and exponential fins. They discovered that

31 January 2024 17:57:00

© Author(s) 2024

if the shape of the fins is exponential, the heat emission will be higher. By varying the shape, material, and thickness of the fins, Nirrop[2] studied the heat transfer of the cylindrical fin. The Finite Volume Method (FVM) was employed by Sheikholeslami *et al.*[3] to study two-dimensional melting with various fin configurations using a heat exchanger.

Numerous researchers have investigated the heat transfer characteristics of permeable fins under the stimulus of magnetic fields and thermal radiation emphasizing the significance of variable thermal conductivity for practical applications. Patel and Meher[4] examined the temperature distribution, effectiveness, and efficiency of a longitudinal rectangular porous fin. A comprehensive study on the thermal aspects of porous fins with constant and variable thermal conductivities was conducted by Cuce and Cuce[5] and Subray *et al.*[6]

In a numerical study, Madhura *et al.*[7] analyzed the rate of heat emission from a longitudinal porous fin in the presence of Lorentz force, thermal radiation, and variable thermal coefficients and determined that fins can be cooled down easily by controlling the Hartman number and the radiation emission. In another study, Haldar *et al.*[8] investigated the properties of induced convection and natural convection on the heat transfer properties of pin fins made of brass and aluminum. Singh *et al.*[9] conducted an investigational study on quadrangular micro-pin-fin heat sinks to determine the optimal pin-fin shape for forced convection heat removal applications. Khetib *et al.*[10] investigated the cooling of electronic components using cylindrical pin fins and studied the variations in pressure drops and heat transfer by changing the pin fin diameter.

In the early 1940s, Gardner[11] first proposed spine fin profiles by considering the approximate value of the Bessel function and developed an ordinary differential equation for spines. The study by Holtzapple *et al.*[12] was the first to determine the fin's efficiency by assuming that the fin has a constant cross-section area. Carranza[13] studied the spine by the finite difference method with the same geometry considered by Holtzapple, but he assumed that the spine is pyramidal. It was discovered that the productivity of the spine fin is greatly diverse by considering either a constant or variable cross-sectional area. Fallo *et al.*[14] investigated the heat transfer in a cylindrical spine fin with the impact of variable thermal conductivity and heat transfer coefficient using the three-dimensional differential transform method to solve the partial differential equation.

Nawaz *et al.*[15] conducted an experimental evaluation of the heat transfer rate of an oriented square-shaped pin-fin heat sink using graphene oxide nanofluid and fluctuating physical parameters. Their study revealed that the use of graphene oxide nanofluid resulted in an enhancement of the heat sink's thermal performance. Fayyaz *et al.*[16] worked on different configurations (square and triangular) of pin-fin heat sinks using numerical models, both with and without Phase Change Material (PCM). Finally, they noticed that the square spine fin heat sink reduces the temperature more than the triangular pin fin, which is due to the difference in surface area. Babar *et al.*[17] empirically deliberated the thermic study of a heat sink by changing the position of air-foil-shaped pin fins.

The examination of heat transfer in a porous medium in spine fin has become more significant over the past few decades due to its industrial applications such as room air conditioners, package terminal air conditioners, and central heating and cooling units. From the overview of the above literature, very limited research has been carried out related to spine fin. In light of these facts, the current research presents a study of the transfer of heat in porous spine pins with copper, MoS_4, and water hybrid nanofluid. Natural conduction, variable thermal conductivity, magnetic field, and radiation heat transfer processes are taken into account as novel features for the thermal analysis of the porous spine fin with a hybrid nanofluid. The Finite Difference Method (FDM) and differential transform method (DTM) are used to solve energy equations for both cylindrical and concave parabolic profiles, and the resulting findings are described graphically and in tabular form.

II. PROBLEM FORMULATION

Figure 1(a) shows the arbitrary shape of a spine fin. The fin has a base temperature of T_b and is exposed to an ambient temperature of T_a. The single-phase fluid is considered isotropic, homogeneous, and fully saturated within the porous matrix. The Darcy model describes the relationship between the fluid and porous media. The temperature is assumed to be constant throughout the thickness of the fin, and the fluid and porous matrix are in thermal equilibrium with constant physical properties. A magnetic field is applied in the y-direction, and the local heat transfer coefficient $\boldsymbol{h}$ is assumed to be constant along the surface of the fin. The thermal conductivity of the fin varies linearly with temperature,

$$Q_x - Q_{x+dx} = \left[\begin{array}{c} 2hPf_2(x)(T-T_a)dx + m_f(C_p)_{hnf}(T-T_a) + \varepsilon P\sigma\left(T^4 - T_a{}^4\right)dx \\ + \dfrac{J_c \times J_c}{\sigma_{hnf}}(T-T_a)dx \end{array}\right], \tag{1}$$

where $J_c = \sigma_f(E + V \times B)$ is the power of conduction current and

$$\frac{J_c \times J_c}{\sigma_{hnf}} = \sigma_{hnf} B_0^2 u^2.$$

The fluid's mass flow rate through a permeable medium is given by

$$m_f = \rho v_w w dx. \tag{2}$$

From Darcy's model, v_w through a permeable medium is considered as

$$v_w = \frac{g k_f K \rho \beta}{\mu_f}(T - T_a). \tag{3}$$

The expression for the energy flux vector of conduction and radiation near the base of the spine is given by

31 January 2024 17:57:00

© Author(s) 2024

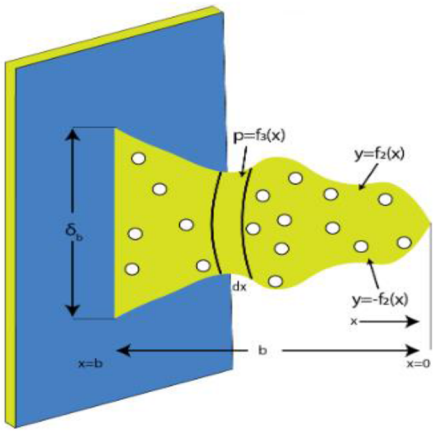

Fig. 1(a). Spine fin with arbitrary profile.

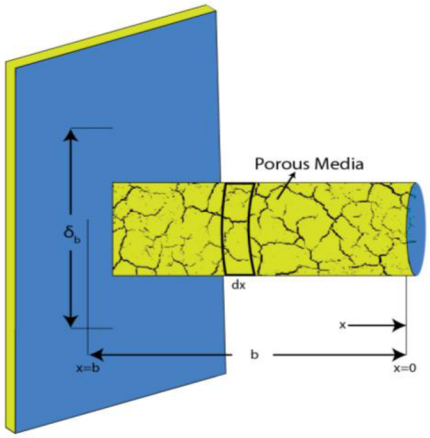

Fig. 1(b): Cylindrical spine.

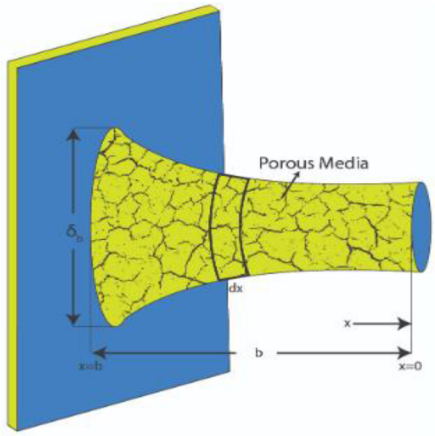

Fig. 1(c): Concave parabolic profile

FIG. 1. (a) Spine fin with arbitrary profile. (b) Cylindrical spine. (c) Concave parabolic profile.

$$Q_{base} = Q_{conduction} + Q_{radiation}, \tag{4}$$

and $Q_{conduction}$ from Fourier's law is given by

$$Q_{conduction} = -[f_2(x)]^2 k_{hnf}(T)\frac{dT}{dx}. \tag{5}$$

The variable thermal conductivity is given by

$$k_{hnf}(T) = k_{hnf}(1 + \lambda(T - T_a)).$$

By substituting Eqs. (2)–(5) in Eq. (1), we get

$$\frac{d}{dx}\left[k_{hnf}(1 + \lambda(T - T_a))[f_2(x)]^2\frac{dT}{dx}\right] = \left[\begin{array}{c} 2hPf_2(x)(T - T_a) + \dfrac{Kg(\rho C_p)_{hnf}(\rho\beta)_{hnf}wk_f}{\mu_{hnf}}(T - T_a)^2 \\ +\varepsilon P\sigma\left(T^4 - T_a^{\,4}\right) + \sigma_{hnf}B_0^2u^2(T - T_a) \end{array}\right]. \tag{6}$$

Depending on how the thickness of the fin changes along its length, the spine fin can be classified into various profiles. For the present investigation, two different profiles are chosen.

- Cylindrical profile: The profile function of the cylindrical spine is shown in Fig. 1(b), and it can be expressed as

$$f_2(x) = \left(\frac{\delta_b}{2}\right). \tag{7}$$

- Concave parabolic profile: The profile function of the concave parabolic profile is shown in Fig. 1(c), and it can be expressed as

$$f_2(x) = \left(\frac{\delta_b}{2}\right)\frac{x}{b}. \tag{8}$$

The boundary condition for the fin tip is given as follows:

$$x = 0, \quad T(0) = T_b,$$

at

$$x = b, \quad \frac{dT(b)}{dx} = 0. \tag{9}$$

The following are the dimensionless parameters:

$$\theta = \frac{T - T_a}{T_b - T_a},\ X = \frac{x}{b},\ \beta = \lambda(T_b - T_a),\ M = \frac{8hPb^2}{\delta_b{}^2k_f},$$

$$S_H = \frac{4g(\rho\beta)_f(\rho C_p)_f k_f b^2 Kw}{\delta_b{}^2 Zk_f\mu_f}(T_b - T_a),$$

$$Nr = \frac{4\varepsilon\sigma Pb^2(T_b - T_a)^3}{\delta_b{}^2k_f},\ H = \frac{4\sigma_f b^2B_0^2u^2}{\delta_b{}^2k_f},\ Nt = \frac{T_a}{(T_b - T_a)}.$$

By considering the above dimensionless parameters and properties in Table I, Eq. (6) changes as follows:

31 January 2024 17:57:00

© Author(s) 2024

TABLE I. Thermophysical properties of hybrid nanofluid.[18]

Properties	Expressions for hybrid nanofluid
Dynamic viscosity	$\mu_{hnf} = \mu_f\left[(1-\phi_1)^{-2.5}(1-\phi_2)^{-2.5}\right]$
Thermal conductivity	$k_{hnf} = k_{nf}\left(\frac{k_{s2}+(q-1)k_{nf}-(q-1)\phi_2(k_{nf}-k_{s2})}{k_{s2}+(q-1)k_{nf}+\phi_2(k_{nf}-k_{s2})}\right)$, where $k_{nf} = k_f\left(\frac{k_{s1}+(q-1)k_f-(q-1)\phi_1(k_f-k_{s1})}{k_{s1}+(q-1)k_f+\phi_1(k_f-k_{s1})}\right)$
Electrical conductivity	$\sigma_{hnf} = \sigma_{nf}\left(\frac{\sigma_{s2}+2\sigma_{nf}-2\phi_2(\sigma_{nf}-\sigma_{s2})}{\sigma_{s2}+2\sigma_{nf}+\phi_2(\sigma_{nf}-\sigma_{s2})}\right)$, where $\sigma_{nf} = \sigma_f\left(\frac{\sigma_{s1}+2\sigma_f-2\phi_1(\sigma_f-\sigma_{s1})}{\sigma_{s1}+2\sigma_f+\phi_1(\sigma_f-\sigma_{s1})}\right)$
Heat capacity	$(\rho C_p)_{hnf} = (\rho C_p)_f(1-\phi_2)\left[(1-\phi_1)+\phi_1\frac{(\rho C_p)_{n1}}{(\rho C_p)_f}\right]+\phi_2\frac{(\rho C_p)_{n2}}{(\rho C_p)_f}$
Thermal expansion	$(\rho\beta)_{hnf} = \left[(1-\phi_1)(\rho\beta)_f+\phi_1(\rho\beta)_{s1}\right](1-\phi_2)+\phi_2(\rho\beta)_{s2}$

- For cylindrical profile

$$(1+\beta\theta)\frac{d^2\theta}{dX^2}+\beta\left(\frac{d\theta}{dX}\right)^2-\frac{1}{Z}\left(M\theta+Z_2S_H\theta^2+Nr\left((\theta+Nt)^4-(Nt)^4\right)+Z_1H\theta\right)=0. \tag{10}$$

- For concave parabolic profile

$$\left(\beta X^4\left(\frac{d\theta}{dX}\right)^2+(1+\beta\theta)X^4\frac{d^2\theta}{dX^2}+(1+\beta\theta)4X^3\frac{d\theta}{dX}\right)-\frac{1}{Z}\left(\begin{array}{l}M\theta+Z_2S_H\theta^2+Z_1H\theta\\+Nr\left((\theta+Nt)^4-(Nt)^4\right)\end{array}\right)=0. \tag{11}$$

The following are the non-dimensionalized boundary constraints:

$$X=0,\ \ \theta(0)=1,$$

at

$$X=1,\ \ \theta'(1)=0. \tag{12}$$

III. PROBLEM SOLUTION

The fluid flow problems are solved by using various numerical schemes, see Refs. 19–26. For the present study, we consider the following schemes:

A. Finite difference approximation

- Cylindrical profile

$$\theta_{i-1}(1+\beta\theta_i)+\theta_i\left[\begin{array}{l}\beta\theta_i-2\beta\theta_{i+1}-2-2\beta\theta_i+\beta\theta_{i+1}+Z_1H\\-\frac{h^2}{Z}\left(\begin{array}{l}M+Z_2S_H\theta_i+Nr{\theta_i}^3+6Nr(Nt)^2\theta_i\\+4Nr{\theta_i}^2Nt+4Nr(Nt)^3\end{array}\right)\end{array}\right]+\theta_{i+1}(\beta\theta_{i+1}+1)=0. \tag{13}$$

- Concave parabolic profile

$$\theta_{i-1}\left(\begin{array}{l}{X_i}^4+\\\beta\theta_i{X_i}^4\end{array}\right)+\theta_i\left[\begin{array}{l}\left(\begin{array}{l}\beta{X_i}^4\theta_i-2\beta{X_i}^4\theta_{i+1}-2{X_i}^4-2\beta\theta_i{X_i}^4\\+\beta{X_i}^4\theta_{i+1}-4{X_i}^3h+4\beta{X_i}^3h\theta_{i+1}\\+Z_1H-4\beta{X_i}^3h\theta_i\end{array}\right)\\-\frac{h^2}{Z}\left(M+Z_2S_H\theta_i+Nr\left(\begin{array}{l}{\theta_i}^3+6(Nt)^2\theta_i\\+4{\theta_i}^2Nt+4(Nt)^3\end{array}\right)\right)\end{array}\right]+\theta_{i+1}\left(\begin{array}{l}\beta{X_i}^4\theta_{i+1}\\+{X_i}^4+4{X_i}^3h\end{array}\right)=0. \tag{14}$$

31 January 2024 17:57:00

© Author(s) 2024

B. Differential transform method

The transformed boundary conditions are

$$\Theta(0) = 1 \text{ and } \sum_{i=0}^{\infty} \Theta(i) = 0. \tag{15}$$

Considering initial values $\Theta(1) = a$, Eqs. (13) and (14) with modified boundary constraints are used to solve a system of algebraic calculations and determine the unknown "a." The obtained solutions are given below.

- Cylindrical profile

$$\left[\begin{array}{l} \left(\begin{array}{l} \beta\sum_{i=0}^{k}(i+1)\Theta(i+1)(k-i+1)\Theta(k-i+1)+(k+1)(k+2)\Theta(k+2) \\ +\beta\sum_{i=0}^{k}\Theta(i)(k-i+1)(k-i+2)\Theta(k-i+2) \end{array}\right) \\ -\frac{1}{Z}\left(\begin{array}{l} M\Theta(k)+Z_2S_H\sum_{i=0}^{k}\Theta(i)\Theta(k-i)+Nr\sum_{i=0}^{k}\sum_{m=0}^{i}\sum_{n=0}^{m}\Theta(n)\Theta(k-i)\Theta(i-m)\Theta(m-n) \\ +6Nr(Nt)^2\sum_{i=0}^{k}\Theta(i)\Theta(k-i)+4NrNt\sum_{i=0}^{k}\sum_{m=0}^{i}\Theta(m)\Theta(k-i)\Theta(i-m) \\ +4Nr(Nt)^3\Theta(k)+Z_1H\Theta(k) \end{array}\right) \end{array}\right] = 0. \tag{16}$$

The solutions are

$$\Theta[2] = \frac{M+Nr+4NrNt+6NrNt^2+4NrNt^3-a^2Z\beta+Z_2S_H+HZ_1}{2Z(1+\beta)},$$

$$\Theta[3] = \frac{aM+4aNr+12aNrNt+12aNrNt^2+4aNrNt^3+2aZ_2S_H+aHZ_1-6aZ\beta\Theta[2]}{6Z(1+\beta)},$$

$$\Theta[4] = \frac{1}{12Z(1+\beta)}\left(\begin{array}{l} 6a^2Nr+12a^2NrNt+6a^2NrNt^2+a^2Z_2S_H+M\Theta[2]+4Nr\Theta[2]+12NrNt\Theta[2] \\ +12NrNt^2\Theta[2]+4NrNt^3\Theta[2]+2S_H\Theta[2]+HZ_1\Theta[2]-6Z\beta\Theta[2]^2-12aZ\beta\Theta[3] \end{array}\right),$$

and so on.

31 January 2024 17:57:00

© Author(s) 2024

- Concave parabolic profile

$$\left[\begin{array}{l}\left(\begin{array}{l}\beta\sum_{i=0}^{k}(i+1)\Theta(i+1)(k-i+1)\Theta(k-i+1)+\frac{1}{2}\left(\begin{array}{l}\sum_{i=0}^{k}\delta(i+1)(k-i+1)\Theta(k-i+1)\\+(k+1)(k+2)\Theta(k+2)\end{array}\right)\\+\frac{1}{2}\beta\sum_{i=0}^{k}\sum_{m=0}^{i}\delta(i+1)\Theta(k-i)(k-i-m+1)\Theta(k-i-m+1)\\+\beta\sum_{i=0}^{k}\Theta(i)(k-i+1)(k-i+2)\Theta(k-i+2)+2\sum_{i=0}^{k}\delta(i+1)(k-i+1)\Theta(k-i+1)\\+\beta\sum_{i=0}^{k}\sum_{m=0}^{i}\delta(i+1)\Theta(k-i)(k-i-m+1)\Theta(k-i-m+1)\end{array}\right)\\-\frac{1}{Z}\left(\begin{array}{l}\frac{1}{4}M\sum_{i=0}^{k}\delta(i+3)\Theta(k-i)+\frac{1}{4}Z_2S_H\sum_{i=0}^{k}\sum_{m=0}^{i}\delta(i+3)\Theta(k-i)\Theta(i-m)\\+\frac{1}{4}Nr\sum_{i=0}^{k}\sum_{m=0}^{i}\sum_{n=0}^{m}\sum_{s=0}^{n}\delta(i+3)\Theta(k-i)\Theta(i-m)\Theta(m-n)\Theta(n-s)\\+\frac{3}{2}Nr(Nt)^2\sum_{i=0}^{k}\sum_{m=0}^{i}\delta(i+3)\Theta(k-i)\Theta(i-m)\\+NrNt\sum_{i=0}^{k}\sum_{m=0}^{i}\sum_{n=0}^{m}\delta(i+3)\Theta(k-i)\Theta(i-m)\Theta(m-n)\\+Nr(Nt)^3\sum_{i=0}^{k}\delta(i+3)\Theta(k-i)+\frac{1}{4}Z_1H\sum_{i=0}^{k}\delta(i+3)\Theta(k-i)\end{array}\right)\end{array}\right]=0. \tag{17}$$

The solutions are

$$\Theta[2]=-\frac{a^2\beta}{2(1+\beta)},$$

$$\Theta[3]=\frac{-5a-3a\beta-12a\beta\Theta[2]}{12(1+\beta)},$$

$$\Theta[4]=\frac{-3a^2\beta-10\Theta[2]-6a\beta\Theta[2]-12\beta\Theta[2]^2-24a\beta\Theta[3]}{24(1+\beta)},$$

$$\Theta[5]=\frac{1}{80Z(1+\beta)}\left(\begin{array}{l}M+Nr+3aNr+3a^2Nr+a^3Nr+4NrNt+8aNrNt+4a^2NrNt+6NrNt^2\\+6aNrNt^2+4NrNt^3+Ra+aRa+HNrZ_1+3Nr\Theta[2]+6aNr\Theta[2]\\+8NrNt\Theta[2]+8aNrNt\Theta[2]+6NrNt^2\Theta[2]+Ra\Theta[2]-12Z\beta\Theta[2]^2\\+3Nr\Theta[3]+8NrNt\Theta[3]+6NrNt^2\Theta[3]+Ra\Theta[3]-30Z\Theta[3]\\-98Z\beta\Theta[2]\Theta[3]-80aZ\beta\Theta[4]\end{array}\right),$$

and so on.

By substituting the cylindrical profile Θ values in the source equation of DTM, it can be obtained that the closed form of the solutions is

$$\Theta(X)=a+\Theta(2)X^2++\Theta(3)X^3+\Theta(4)X^4+\cdots. \tag{18}$$

By substituting Eqs. (15) into (18) in point $X=1$, the values of "***a***" can be obtained.

- For cylindrical profile

$$\Theta(1)=\left(\begin{array}{l}a+\frac{M+Nr+4NrNt+6NrNt^2+4NrNt^3-a^2Z\beta+Z_2S_H+HZ_1}{2Z(1+\beta)}\\+\frac{aM+4aNr+12aNrNt+12aNrNt^2+4aNrNt^3+2aZ_2S_H+aHZ_1-6aZ\beta\Theta[2]}{6Z(1+\beta)}+\cdots\end{array}\right)=0. \tag{19}$$

31 January 2024 17:57:00

© Author(s) 2024

TABLE II. Computational values of base fluids and nanoparticles.

Properties	Base fluid (H_2O)	Cu	MoS_4
C_p (J/kgK)	4179	385	397.21
ρ (kg/m^2)	997.1	8933	5060
k (W/mK)	0.6130	400	904.4
σ (Simens/m)	5.5×10^{-6}	59.6×10^{6}	2.09×10^{4}
β (1/K)	21	1.67×10^{-5}	2.8424×10^{-5}

To obtain the value of "a," Eq. (18) needs to be solved using the MATLAB software for the given boundary conditions and physical parameters. The same procedure is then repeated for the concave parabolic profile.

IV. RESULTS AND DISCUSSION

In this study, the ordinary nonlinear equations with temperature-dependent variable thermal conductivity, Lorentz force, radiation effect, and permeable media are solved by using the differential transform method and the finite difference method. By considering values in Table II, all the points are plotted.

A. Comparison study

The validation of the DTM and FDM results for two profiles at $M = 2$, $Nr = 2$, $H = 2$, $Nt = 0.4$, $S_H = 2$, and $\beta = 0.2$ is shown in Table II. DTM results agreed with FDM results. Based on the information provided in Table III, it can be inferred that the differential transform method (DTM) is a suitable technique for solving both linear and nonlinear equations.

B. Parametric study

Figure 2 shows the effect of hybrid and nanofluids on the temperature profile. This graph shows more heat transfer enhancement with a hybrid nanofluid than a nanofluid alone due to the thermal conductivity of two nanoparticles. Due to this, the complete study is carried out on a hybrid nanofluid. The temperature of the concave parabolic profile is greater than that of the cylindrical profile because T_b for the concave parabolic profile is greater than that of the cylindrical profile.

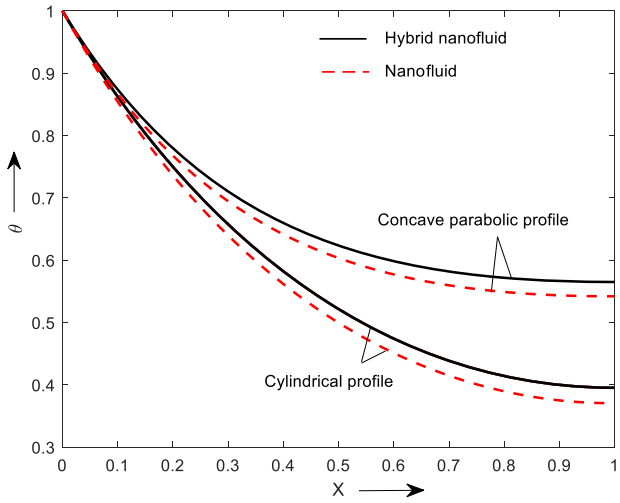

FIG. 2. Temperature graph of both profiles for hybrid nanofluid and nanofluid.

Figure 3 offers the impact of the radiation parameter on the temperature distribution profile, revealing that the rate of heat transmission of the fin decreases as the radiation parameter surges. Physically, the radiation parameter effectively regulates the fin temperature and significantly subsidizes the system cooling. The shape of the nanoparticles plays a significant role and is observed most for the cylinder-shaped nanoparticles.

Figure 4 explains the impact of the porosity parameter on the temperature profile. As the porosity parameter increases, the thermal performance decreases. This is because an increase in the porosity causes a decrease in the effective thermal conductivity of the permeable fin due to the exclusion of solid material. The temperature of the cylinder-shaped nanoparticles is higher than that of the brick-shaped nanoparticles. In addition, the concave parabolic profile exhibits a higher rate of heat transfer.

TABLE III. Comparison table between numerical (FDM) and semi-analytical method (DTM).

	Cylindrical profile				Concave parabolic profile			
X	FDM		DTM		FDM		DTM	
⋯	q = 3.7	q = 4.9	q = 3.7	q = 4.9	q = 3.7	q = 4.9	q = 3.7	q = 4.9
0.1	0.867 984	0.874 026	0.867 984	0.874 026	0.873 794	0.890 88	0.873 794	0.890 88
0.2	0.747 937	0.7725	0.747 937	0.7725	0.787 824	0.809 279	0.787 824	0.809 279
0.3	0.641 956	0.684 918	0.641 956	0.684 918	0.710 103	0.743 837	0.710 103	0.743 837
0.4	0.579 127	0.621 588	0.579 127	0.621 588	0.655 294	0.701 202	0.655 294	0.701 202
0.5	0.514 943	0.564 269	0.514 943	0.564 269	0.620 41	0.670 773	0.620 41	0.670 773
0.6	0.460 382	0.511 494	0.460 382	0.511 494	0.600 39	0.649 698	0.600 39	0.649 698
0.7	0.426 811	0.485 085	0.426 811	0.485 085	0.580 41	0.635 789	0.580 41	0.635 789
0.8	0.398 025	0.457 578	0.398 025	0.457 578	0.570 807	0.627 369	0.570 807	0.627 369
0.9	0.381 769	0.446 898	0.381 769	0.446 898	0.566 01	0.623 158	0.566 01	0.623 158

31 January 2024 17:57:00

© Author(s) 2024

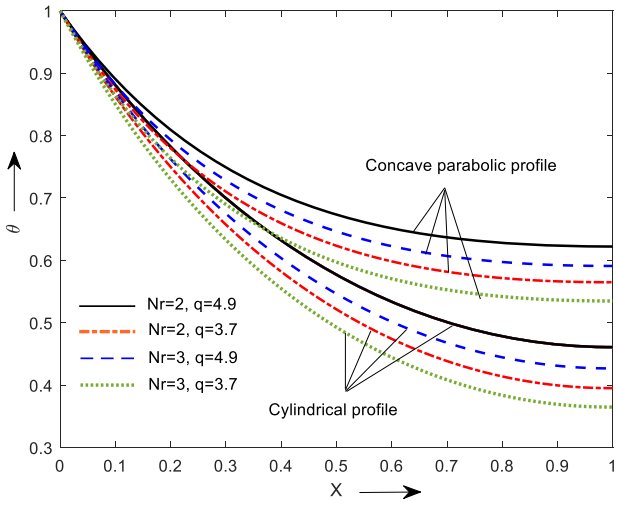

FIG. 3. Temperature distribution of both profiles for different values of Nr.

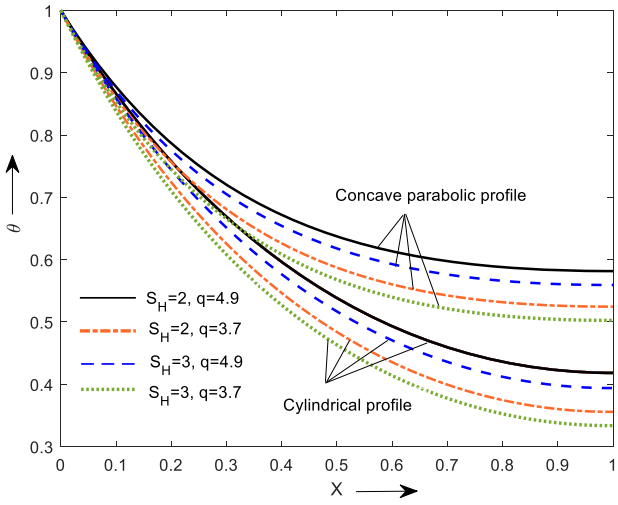

FIG. 4. Temperature dispersal for various values of S_H.

The influence of the Hartmann number on θ for both the concave parabolic and cylindrical profiles is presented in Fig. 5. It is observed that the temperature decreases as the Hartmann number increases. This phenomenon is caused due to the magnetic force becoming stronger with increasing Hartmann number, which suppresses the convective heat transfer mechanism and enhances the overall heat transfer of the fin. Furthermore, the presence of the Lorentz force amplifies the impact of the buoyant force, resulting in increased convective heat transfer. As a result, the rate of heat emission is higher for the concave parabolic fin than for the cylindrical profile.

The impact of the variable thermal conductivity on temperature θ can be observed in Fig. 6. The temperature upsurges with

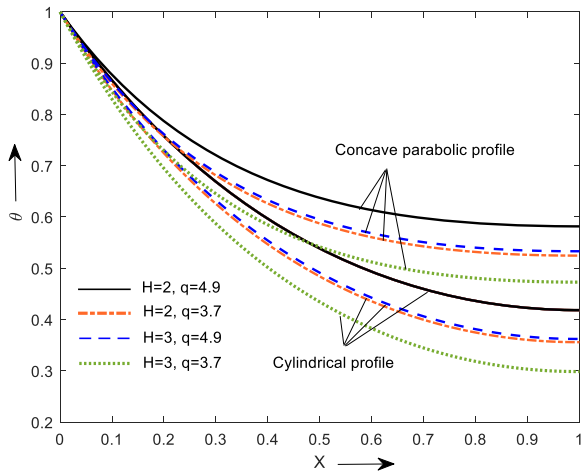

FIG. 5. Temperature distribution for various values of H.

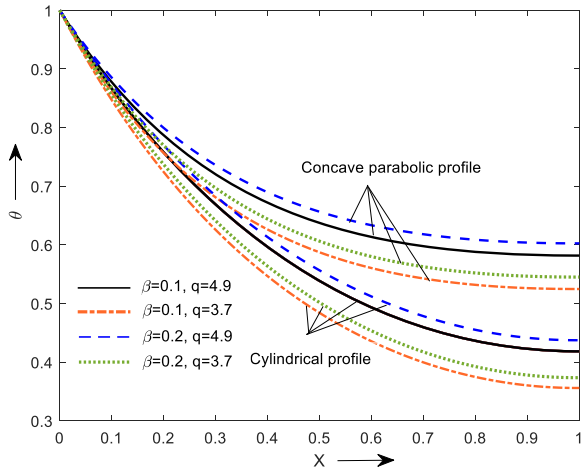

FIG. 6. Temperature distribution for various values of β.

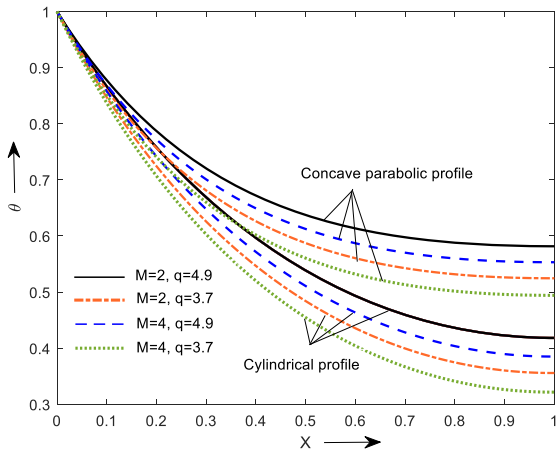

FIG. 7. Temperature distribution for various values of *M*.

31 January 2024 17:57:00

© Author(s) 2024

increasing values β. This is caused by higher values of β since with an increase in heat conduction through fins, the temperature in the fin likewise increases. Figure 7 reveals the impact of M on θ for both cylindrical and concave parabolic profiles. As the value of the conductive parameter increases, the thermal distribution through the fin decreases gradually. Physically, when convection becomes stronger, the material's temperature decreases, increasing the efficiency of the cooling process.

V. CONCLUSION

The thermal case study is carried out to investigate the consideration of both cylindrical and concave parabolic profiles for spine fins in a hybrid nanofluid. The flow field is manifested with a magnetic field and temperature-dependent thermal conductivity. The flow is mathematically modeled and solved by using analytical and numerical schemes. The key outcomes of the present analysis are as follows:

- Hybrid nanofluid enhances the flow field temperature more than the nanofluid.
- The fin's heat transfer rate decreases when the porous medium is considered.
- Increasing the thermal conductivity of the fin improves its thermal performance.
- The temperature profile increases toward higher values of radiation parameter.
- The fin geometry and radiation parameter decrease the thermal performance of the fin.
- A concave parabolic profile admits a higher enhancement in temperature than a cylindrical profile.

ACKNOWLEDGMENTS

The authors acknowledge Prince Sultan University, Saudi Arabia, for the technical support through the TAS research lab.

AUTHOR DECLARATIONS

Conflict of Interest

The authors have no conflicts to disclose.

Author Contributions

Tanuja T. N.: Conceptualization (equal); Data curation (equal); Formal analysis (equal); Investigation (equal). **Kavitha L**: Conceptualization (equal); Data curation (equal); Methodology (equal); Validation (equal); Writing – original draft (equal). **Khalil Ur Rehman**: Formal analysis (equal); Methodology (equal); Validation (equal); Writing – original draft (equal). **G. V. Kumar**: Resources (equal); Software (equal); Supervision (equal); Validation (equal). **Wasfi Shatanawi**: Conceptualization (equal); Data curation (equal); Methodology (equal); Supervision (equal). **S. V. K. Varma**: Conceptualization (equal); Formal analysis (equal); Methodology (equal); Software (equal). **Zeeshan Asghar**: Resources (equal); Validation (equal); Visualization (equal).

DATA AVAILABILITY

The datasets generated during and/or analyzed during the current study are available from the corresponding authors on reasonable request.

REFERENCES

[1] A. Moradi and H. Ahmadikia, "Analytical solution for different profiles of fin with temperature-dependent thermal conductivity," Math. Probl. Eng. **2010**, 1–15.
[2] R. B. N. Niroop Kumar, "Calculating heat transfer rate of cylinder fins body by varying geometry and material," Int. J. Mech. Eng. Rob. Res. **3**(4), 642–657 (2014).
[3] M. Sheikholeslami, M. Jafaryar, A. Shafee, and Z. Li, "Simulation of nanoparticles application for expediting melting of PCM inside a finned enclosure," Physica A **523**, 544–556 (2019).
[4] T. Patel and R. Meher, "A study on temperature distribution, efficiency and effectiveness of longitudinal porous fins by using adomian decomposition sumudu transform method," Procedia Eng. **127**, 751–758 (2015).
[5] E. Cuce and P. M. Cuce, "A successful application of homotopy perturbation method for efficiency and effectiveness assessment of longitudinal porous fins," Energy Convers. Manage. **93**, 92–99 (2015).
[6] P. V. Ananth Subray, B. N. Hanumagowda, S. V. K. Varma, A. M. Zidan, M. Kbiri Alaoui, C. S. K. Raju, N. A. Shah, and P. Junsawang, "Dynamics of heat transfer analysis of convective-radiative fins with variable thermal conductivity and heat generation: Differential transformation method," Mathematics **10**, 3814 (2022).10.3390/math10203814
[7] K. R. Madhura, Babitha, G. Kalpana, and O. D. Makinde, "Thermal performance of straight porous fin with variable thermal conductivity under magnetic field and radiation effects," Heat Transfer **49**(8), 5002–5019 (2020).
[8] R. Haldar, A. Kumar, T. Janah, and P. Biswas, "Experimental investigation of heat transfer by forced and natural convection in a pin fin for different materials," Int. J. Res. Appl. Sci. Eng. Technol. **10**(2), 1254–1260 (2022).
[9] N. R. Singh, S. Onkar, and J. Ramkumar, "Thermo-hydraulic performance of square micro pin fins under forced convection," Int. J. Heat Technol. **39**(1), 170–178 (2021).
[10] Y. Khetib, A. Alahmadi, A. Alzaed, S. M. Sajadi, R. Vaziri, and M. Sharifpur, "Sensitivity of pin-fin configuration to pin diameter: Heat transfer enhancement," Chem. Eng. Commun. **210**(5), 655–669 (2023).
[11] K. A. Gardner, "Efficiency of extended surface," J. Fluids Eng. **67**(8), 621–628 (1945).
[12] M. T. Holtzapple, K. Lin, and A. L. Allen, "Heat transfer and pressure drop of spined pipe in cross-flow—Part II," Heat Transfer Stud. ASHRAE Trans. 96(2), 5167679 (1990).
[13] R. G. Carranza, "Spine fin efficiency of spined pipe heat exchangers," in National Heat Transfer Conference Proceedings, Atlanta, 1993.
[14] N. Fallo, R. J. Moitsheki, and O. D. Makinde, "Analysis of heat transfer in a cylindrical spine fin with variable thermal properties," Defect Diffus. Forum **387**, 10–22 (2018).
[15] S. Nawaz, H. Babar, H. M. Ali, M. U. Sajid, M. M. Janjua, Z. Said, A. K. Tiwari, L. Syam Sundar, and C. Li, "Oriented square shaped pin-fin heat sink: Performance evaluation employing mixture based on ethylene glycol/water graphene oxide nanofluid," Appl. Therm. Eng. **206**, 118085 (2022).
[16] H. Fayyaz, A. Hussain, and T. Bin Irshad, "Numerical investigation of different configurations of pin fin heat sinks with and without PCM," in ICAME-22 (Engineering Proceedings, 2022), p. 22.
[17] H. Babar, H. Wu, H. M. Ali, and W. Zhang, "Hydrothermal performance of inline and staggered arrangements of airfoil shaped pin-fin heat sinks: A comparative study," Therm. Sci. Eng. Prog. **37**, 101616 (2023).
[18] S. Kavya, V. Nagendramma, N. A. Ahammad, S. Ahmad, C. S. K. Raju, and N. A. Shah, "Magnetic-hybrid nanoparticles with stretching/shrinking cylinder in a suspension of MoS_4 and copper nanoparticles," Int. Commun. Heat Mass Transfer **136**, 106150 (2022).

31 January 2024 17:57:00

© Author(s) 2024

[19]A. Kamran and E. Azhar, "Numerical outlook of a viscoelastic nanofluid in an inclined channel via Keller box method," Int. Commun. Heat Mass Transfer **137**, 106260 (2022).
[20]D. Habib, N. Salamat, S. H.. Abdal, and B. Ali, "Numerical investigation for MHD Prandtl nanofluid transportation due to a moving wedge: Keller box approach," Int. Commun. Heat Mass Transfer **135**, 106141 (2022).
[21]Y. Xia, S. Wei, Y. Deng, and Y. Jin, "A new enriched method for extended finite element modeling of fluid flow in fractured reservoirs," Comput. Geotech. **148**, 104806 (2022).
[22]M. J. Li, Y. Lian, and X. Zhang, "An immersed finite element material point (IFEMP) method for free surface fluid–structure interaction problems," Comput. Methods Appl. Mech. Eng. **393**, 114809 (2022).
[23]M. Shoaib Arif, K. Abodayeh, and Y. Nawaz, "A computational scheme for stochastic non-Newtonian mixed convection nanofluid flow over oscillatory sheet," Energies **16**(5), 2298 (2023).
[24]Y. Nawaz, M. S. Arif, and K. Abodayeh, "An unconditionally stable third order scheme for mixed convection flow between parallel plates with oscillatory boundary conditions," Int. J. Numer. Methods Fluids **95**(6), 937–953 (2023).
[25]M. S. Arif, K. Abodayeh, Y. Nawaz, and Y. Nawaz, "Design of finite difference method and neural network approach for casson nanofluid flow: A computational study," Axioms **12**, 527 (2023).
[26]S. Li and Y. I.. Dimitrienko, "Least squares finite element simulation of local transfer for a generalized Newtonian fluid in 2D periodic porous media," J. Non-Newtonian Fluid Mech. **316**, 105032 (2023).

31 January 2024 17:57:00

© Author(s) 2024